Optics & Laser Technology 44 (2012) 1163–1171

Contents lists available at SciVerse ScienceDirect

Optics & Laser Technology

journal homepage: www.elsevier.com/locate/optlastec

Research on the curing performance of UV-LED light based stereolithography

Ruidong Xie, Dichen Li *

State Key Laboratory of Manufacturing Systems Engineering, Xi'an Jiaotong University, Xi'an, PR China

ARTICLE INFO

Article history:
Received 28 November 2010
Accepted 13 September 2011
Available online 9 November 2011

Keywords:
Stereolithography
UV-LED
Power matching

ABSTRACT

The UV-LED light based StereoLithography system (LED–SL) was developed. Because of the kinematic behavior of the mechanical scanning workbench, the exposure at the ends of a single cured line is much greater than that in the middle segment, and hence bone-shaped errors occur, which means that the ends of a cured line have larger sizes than the middle segment. The purpose of this paper is to investigate the curing performance of LED–SL process and eliminate the bone-shaped errors. The effects of acceleration and deceleration motions of the scanner on the shape of a cured line were formulated and the curing equations were presented. The light switching and power matching scanning methods were studied to improve the accuracy of a cured line. The comparison results of different scanning methods indicate that although both of the above two methods can improve accuracy, the latter has higher fabrication efficiency and larger scanning range than the former.

1. Introduction

SL is a layered fabrication process, which builds 3D parts by scanning a focused UV beam over the resin surface, making liquid resin to polymerize into solid [1–4]. The light source must have very high radiance to provide a tightly focused spot on the surface of the photopolymer, which explains the need for a laser [1]. To reduce the cost of Rapid Prototyping (RP) apparatus, new curing light sources have been used to substitute for expensive lasers.

In recent years, high power UV-LEDs have been developed successfully [5]. UV-LEDs exhibit several advantages such as quick response, high monochromaticity, energy conservation, long life, mini-size and inexpensiveness [6,7]. Research work has been carried out to examine the feasibility of using LEDs as the curing light sources [5,6,8,9]. Loose et al. developed a Multiple Photographic Curing system (MPC) with visible LED light sources [10]. An array of multiple beams of LED lights is projected onto the resin surface to build the parts. However, the light power and accuracy are low. And the photopolymer is sensitive to visible light, so a limitation to using MPC is that the photopolymer must be handled in a dark room. Huang and Sung developed a microlithography system with UV-LED sources [7]. Kang and Shin developed a micro-stereolithography system with focused UV-LED light [11]. While the optical power of the LED is less than 40 μW and the diameter of the focused spot is too large.

The LED–SL system, a novel RP apparatus developed by Xi'an Jiaotong University, China, is shown in Fig. 1. LED–SL has a fabrication accuracy of ± 0.2 mm and a normal scanning speed of 500 mm/s, which can meet the needs of ordinary users. And its price and running cost are much lower than laser SL apparatus. The output wavelength of the LED concentrates on 365 nm and coincides with the absorption peak of the resin, so the radiation can be efficiently absorbed for curing. The energy consumption of LED is much lower than that of laser, which conforms to the conception of Green Manufacturing.

For SL process, the basic scanning motion is the reciprocating linear movement of the scanner [12]. When building a single cured line, the scanner always accelerates from a static state to a given speed at the departure end of the line, keeps the given speed in the middle segment, and decelerates to the static state again at the destination end. Compared with the galvanometer scanner of laser SL, the mechanical scanning workbench of LED–SL (Fig. 3) has a low acceleration, so the exposure at the ends of a cured line is much greater than that in the middle segment. Hence, the ends of a line have larger sizes than the middle, which is called bone-shaped errors. The accumulation of bone-shaped errors has an obvious effect on the part accuracy.

In this study, research work was carried out to investigate the curing performance of LED–SL. The effects of acceleration and deceleration motions on the shape of a single cured line were derived from Jacobs' SL principles [1], and the formation of bone-shaped errors was revealed. The light switching and power matching scanning methods were studied to improve the accuracy of a cured line. The light switching method means extending the acceleration and deceleration segments to outside the exposure range, controlling the on-and-off switch of the UV-LED

* Corresponding author.
E-mail addresses: xieruidong2000@yahoo.com.cn, rd.xie@stu.xj (R. Xie), dcli@mail.xjtu.edu.cn (D. Li).

0030-3992/$ - see front matter © 2011 Elsevier Ltd. All rights reserved.
doi:10.1016/j.optlastec.2011.09.019

Fig. 1. LED–SL 350 apparatus.

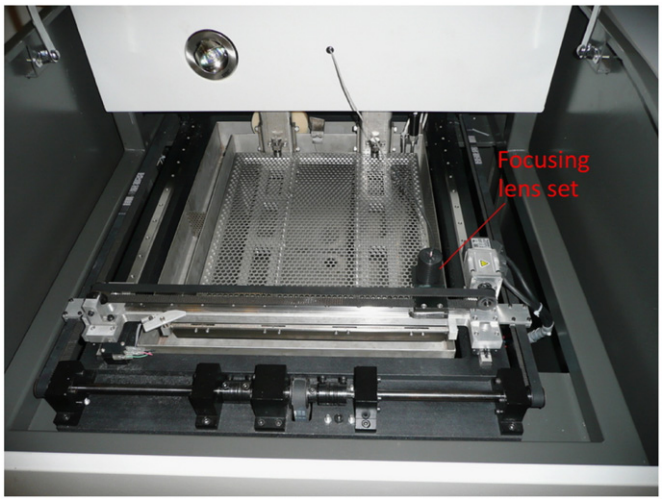

Fig. 3. The two-dimensional workbench.

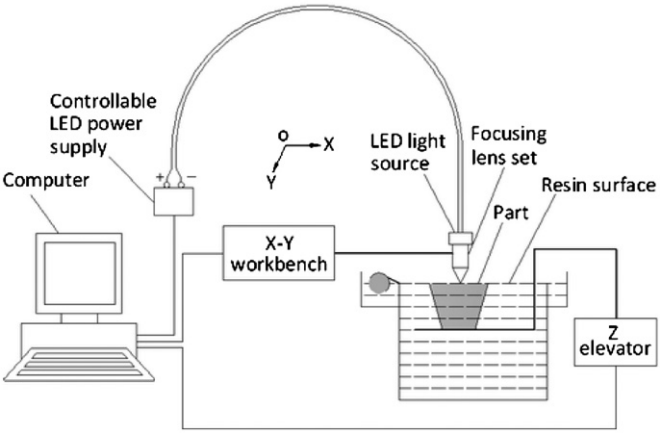

Fig. 2. Schematic diagram of LED–SL.

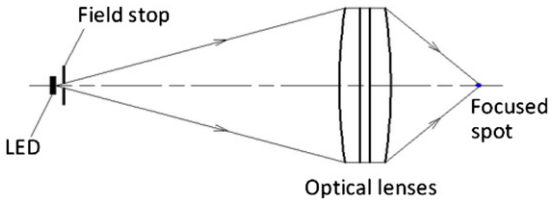

Fig. 4. Focus of the UV-LED light.

power to ensure that only the constant-speed segment of a line is scanned (Figs. 12(b) and 13(b)). The power matching method means dynamically adjusting the beam power to ensure that the power is proportional to the scanning speed (Figs. 12(c) and 13(c)). The different scanning methods were theoretically and experimentally compared.

2. Equipment principle

A LED–SL apparatus is composed of a controlling system, a LED light focusing and switching system, an *X*–*Y* mechanical workbench and a *Z*-axis elevator (Fig. 2). The *X*–*Y* workbench is employed as the driving device of the focusing lens set scanner (Fig. 3). The controlling system, composed of a controlling computer and software, processes the CAD data and controls the fabrication. The LED light focusing and switching system is composed of a NCSU033A P5 high power UV-LED (Nichia corporation, Japan), the focusing lens set, and a controllable LED power supply. The divergent UV light emitted from the LED is focused on the resin surface by the focusing lens set (Fig. 4). The lens set consists of several spherical lenses, and the LED is fixed above the lenses. The UV beam of the LED has a divergence angle of about 120°. However, since limited by the dimension of the lenses, only the light within the range of 30° can be focused. The UV-LED has an end-power of 13.3 mW. The final focal length is 11.2 mm, and the beam waist dimension is 0.42 mm. Controlled by the computer, the workbench drives the scanner to move along *X*–*Y* plane, polymerize the liquid resin according to the current cross-section of a layered part. After the scanning of current layer, the *Z*-axis elevator goes down a layer thickness and the scanning of next layer starts. Stacking up layer by layer, the whole part is fabricated.

The UV-LED has a quick response, and its optical power is proportional to its DC current. Utilizing these advantages, instantaneous switching and real time adjustment of optical power were realized. A controllable LED power supply (Fig. 5) was developed based on an operational amplifier and closed-loop feedback control. Its current output I_{out} is proportional to the analog voltage input from the computer U_{in}. By controlling U_{in}, I_{out} can be dynamically adjusted. The experimentally measured I_{out}–U_{in} curve is shown in Fig. 6, and their mathematical relationship is described in Eq. (1)

$$I_{out} = 0.1U_{in} \tag{1}$$

when U_{in} is 5 V, I_{out} keeps at the rated value 0.5 A; when U_{in} varies within 0–5 V, I_{out} varies within 0–0.5 A in proportion to U_{in}; when U_{in} is 0, the LED is switched off.

3. Experimental methods and results

3.1. Scanning of single cured lines

Single cured lines were scanned using traditional, light switching and power matching methods to compare the extent of bone-shaped errors. The fabrication results are shown in Fig. 7. The fabrication conditions and measurement results are presented in Tables 1 and 2, respectively.